Article

Dehydrophenylnitrenes: Quartet versus Doublet States

Holger F. Bettinger, and Wolfram Sander

J. Am. Chem. Soc., **2003**, 125 (32), 9726-9733• DOI: 10.1021/ja029296u • Publication Date (Web): 19 July 2003

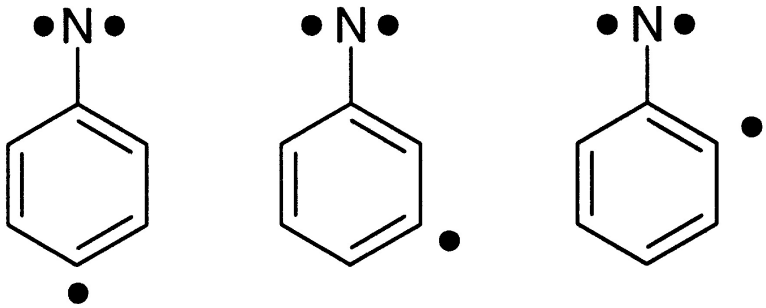

J|A|C|S
ARTICLES
Published on Web 07/19/2003

Dehydrophenylnitrenes: Quartet versus Doublet States

Holger F. Bettinger* and Wolfram Sander

Contribution from the Lehrstuhl für Organische Chemie II, Ruhr-Universität Bochum, Universitätsstrasse 150, 44780 Bochum, Germany

Received November 11, 2002; E-mail: holger.bettinger@ruhr-uni-bochum.de

Abstract: The geometries and energies of 4-, 3-, and 2-dehydrophenylnitrenes (**3**, **4**, and **5**) are investigated using complete active space self-consistent field (CASSCF), multiconfiguration quasi-degenerate second-order perturbation (MCQDPT), and internally contracted multiconfiguration−reference configuration interaction (MRCI) theories in conjunction with a correlation consistent triple-ζ basis set. 4-Dehydrophenylnitrene **3** has a quartet ground state ($^4A_2$). The adiabatic excitation energies to the $^2A_2$, $^2B_2$, $^2A_1$, and $^2B_1$ states are 5, 21, 34, and 62 kcal mol^{-1}, respectively. The $^2B_2$ state has pronounced closed-shell carbene/iminyl radical character, while the lowest-energy $^2B_1$ state is a combination of a planar allene and a 2-iminylpropa-1,3-diyl. The MCQDPT treatment overestimates the excitation energy to $^2B_2$ significantly as compared to CASSCF and MRCI+Q. Among quartet states, $^4A_2$-**3** is the most stable one, while those of **4** and **5** (both $^4A''$) are 3 and 1 kcal mol^{-1} higher in energy. **5** also has a quartet ground state and a $^2A''$ state 7 kcal mol^{-1} higher in energy. On the other hand, the doublet-quartet energy splitting is −6 kcal mol^{-1} for **4** in favor of the doublet state ($^2A''$). Hence, $^2A''$-**4** is the most stable dehydrophenylnitrene, 3.5 kcal mol^{-1} below $^4A_2$ of **3**. The geometry of $^2A''$-**4** shows the characteristic features of through-bond interaction between the in-plane molecular orbitals at N and at C3. The $^2A'$ state of **4** resembles the $^2A_1$ state of **3** and lies 32 kcal mol^{-1} above $^4A''$-**4**. The lowest-energy $^2A'$ state of **5**, on the other hand, resembles the $^2B_2$ state of **3** and lies 22 kcal mol^{-1} above $^4A''$-**5**.

Introduction

Dehydrophenylnitrenes are intriguing species as they unite two reactive and well-investigated motifs: phenylnitrene and phenyl radical. 4-Dehydro-2,3,5,6-tetrafluorophenylnitrene has recently been synthesized in its quartet ground state (**1Q**) by successive photolysis of 2,3,5,6-tetrafluoro-4-iodophenyl azide (**2**) in cryogenic matrixes at 10 K (Scheme 1).[1]

The identification of **1Q** was accomplished by comparison of the measured IR spectrum with that computed at the UB3-LYP/6-311G** level of theory. This computational method places the quartet state about 3 kcal mol^{-1} lower in energy than the lowest-energy doublet state of **1**. These computations also indicated that **1Q** combines aspects of both carbene and nitrene character, as is seen in its two resonance structures (Scheme 2).[1] This dualistic nature is reminiscent of the electronic structure of 4-oxo-2,3,5,6-tetrafluorocyclohexadienylidene, which combines carbene and phenyl/phenoxyl diradical character.[2,3]

The properties of high-spin molecules are currently of enormous interest due to their potential applications in molecular magnets.[4−9] Although the high reactivity of **1** most probably excludes its use in such applications, the investigation of the interplay among the two spin-carrying moieties in dehydrophenylnitrenes and the factors governing the electronic ground states is needed for an understanding of these molecules. We therefore

Scheme 1. Synthesis of 4-Dehydro-2,3,5,6-tetrafluorophenylnitrene (**1**) from 4-Iodo-2,3,5,6-tetrafluorophenyl Azide (**2**) by Stepwise Photolysis in Cryogenic Matrixes at 10 K

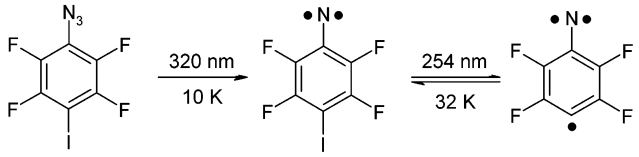

2 **1**

Scheme 2. Resonance Structures of **1** Hint to Its Phenylnitrene/Phenyl Radical (Left) and Carbene/Iminyl Radical (Right) Characters

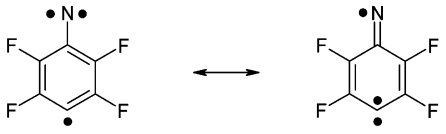

decided to investigate in this paper by multiconfiguration quantum chemical means the parent C_6H_4N 4-, 3-, and 2-dehydrophenylnitrenes (**3**, **4**, and **5**, Chart 1) rather than the perfluorinated species considered in the experimental work. This choice is motivated by the desire to understand the intrinsic properties of the parent systems. Substitution of hydrogen by

(1) Wenk, H. H.; Sander, W. *Angew. Chem.* **2002**, *114*, 2873; *Angew. Chem., Int. Ed.* **2002** *41*, 2742.
(2) Sander, W.; Hübert, R.; Kraka, E.; Gräfenstein, J.; Cremer, D. *Chem.-Eur. J.* **2000**, *6*, 4567.
(3) Wenk, H. H.; Hübert, R.; Sander, W. *J. Org. Chem.* **2001**, *66*, 7994.
(4) Iwamura, H. *Adv. Phys. Org. Chem.* **1990**, *26*, 179.
(5) Iwamura, H. *J. Phys. Org. Chem.* **1998**, *11*, 299.
(6) Dougherty, D. A. *Acc. Chem. Res.* **1991**, *24*, 88.
(7) Rajca, A. *Chem. Rev.* **1994**, *94*, 871.
(8) Miller, J. S., Drillon, M., Eds. *Magnetism: Molecules to Materials*; Wiley-VCH: Weinheim, 2001.

10.1021/ja029296u CCC: $25.00

Chart 1. Labeling of Atomic Positions in Dehydrophenylnitrenes (**3**−**5**), Benzene (**6**), Phenyl Radical (**7**), and Phenylnitrene (**8**) Used in This Work

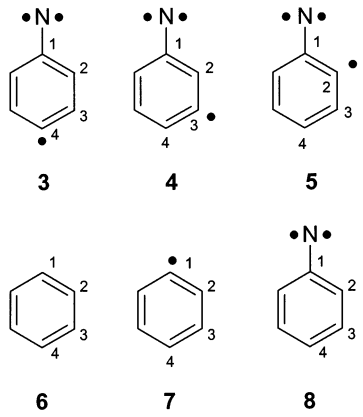

fluorine can be considered a perturbation and modification of the parent, and fluorinated species will be the subject of future work.

Theoretical Methods

All calculations reported here used the triple-ζ correlation consistent basis set of Dunning.[10] The contractions of this basis set read (10s5p2d1f)[4s3p2d1f] for carbon and nitrogen and (5s2p1d)[3s2p1d] for hydrogen. Pure angular momentum basis functions were used throughout in this investigation. The total number of basis functions was 266 for dehydrophenylnitrenes and 280 for phenylnitrene.

The geometries of stationary points were optimized using complete active space self-consistent field (CASSCF) wave functions. The (8,8) active space used for phenylnitrene was identical to that introduced by Borden and co-workers:[11−14] seven π and π^* molecular orbitals (MOs) plus the in-plane p AO centered on nitrogen. The (9,9) active spaces used for dehydrophenylnitrenes comprised these eight phenylnitrene MOs plus the in-plane orbital at the dehydro carbon atom. For 4-dehydrophenylnitrene, we also explored an (11,10) active space which also included the nonbonding electron pair located at nitrogen, but we obtained very similar results for the low energy states considered here. For the description of higher excited states, which are not the subject of this paper, such a larger active space is essential.[15] The active spaces for benzene and the phenyl radical are (6,6) consisting of the six π/π^* MOs and (7,7) including the additional in-plane (a_1) MO, respectively. Finally, for the 2-iminylpropan-1,3-diyl, the four π orbitals and the in-plane b_2 orbital at nitrogen comprised the (5,5) active space. In state-averaged (SA)-CASSCF computations, each of the three states considered contributed equally. The maximum residual Cartesian forces at stationary points were smaller than 0.00001 au. The harmonic vibrational frequencies for the lowest-energy doublet and quartet states were computed by finite differences of analytical gradients. This approach requires reduction of symmetry and thus convergence to the corresponding higher root for higher-lying electronic states. As we were experiencing serious convergence problems in these cases, we computed second derivatives for the lowest-energy states only. To reduce numerical errors, displacements were carried out in two directions for each Cartesian coordinate. The zero-point vibrational energies (ZPVEs) were obtained from unscaled harmonic vibrational frequencies.

The energies were refined by single-point computations using multiconfiguration quasi-degenerate perturbation theory (MCQDPT) to second order.[16,17] As in this work only one specific state is considered at a time, the MCQDPT formalism is equivalent to multireference second-order Møller−Plesset (MRMP2) theory.[18−22] The active spaces of the MRMP2 calculations are identical to those used in the respective geometry optimizations. As second-order perturbation theory based on multiconfiguration wave functions is documented to overestimate the stability of some open-shell relative to closed-shell states,[12,23−25] we attempted internally contracted multiconfiguration−reference configuration interaction computations (MRCI),[26,27] as these are expected to provide a more balanced description of such states. However, we had to reduce the active spaces to the three nonbonding orbitals, as with the larger (9,9) active spaces the computations became prohibitively expensive. Such an approach reduces to conventional singles and doubles CI (CISD) for all quartet states. The coefficients of the (multiconfiguration) reference functions are around 0.905 for all dehydrophenylnitrene states considered. The effects of unlinked quadruple excitations were included via Davidson's correction.[28,29] The core orbitals were kept frozen in all MRMP2 and MRCI computations. The energies mentioned in the text refer to the MRMP2/cc-pVTZ//CASSCF/cc-pVTZ level of theory unless noted otherwise. The MRCI computations used MOLPRO,[30] while all other computations were performed with GAMESS.[31]

Results and Discussion

A. Benzene, Dehydrobenzene (Phenyl Radical), and Phenylnitrene. Before the title species are discussed, a comparison of structural and energetic data computed for benzene (**6**), phenyl radical (**7**), and phenylnitrene (**8**) at the levels of theory employed in the present work (Chart 1, Tables 1 and 2) with experimental and previous computational results is given.

The C−C and C−H bond lengths of benzene are well known from microwave spectroscopy to be r_0(C−C) = 1.3964 ± 0.0002 Å and r_0(C−H) = 1.0831 ± 0.0013 Å.[32] The (6,6)-CASSCF/cc-pVTZ r_e values are 1.392 and 1.073 Å. While the C−C bond lengths are in good agreement with experiment, the C−H bonds, which are not correlated in the computations, are too short. This is in agreement with general observations that the SCF treatment of the inactive space tends to underestimate bond lengths. Upon removal of a hydrogen atom in benzene, the C1−C2 bonds shorten in the resulting phenyl radical **7**

(9) Nau, W. M. *Angew. Chem.* **1997**, *109*, 2551; *Angew. Chem., Int. Ed. Engl.* **1997**, *36*, 2445.
(10) Dunning, T. H. *J. Chem. Phys.* **1989**, *90*, 1007.
(11) Hrovat, D. A.; Waali, E. E.; Borden, W. T. *J. Am. Chem. Soc.* **1992**, *114*, 8698.
(12) Karney, W. L.; Borden, W. T. *J. Am. Chem. Soc.* **1997**, *119*, 1378.
(13) Kemnitz, C. R.; Karney, W. L.; Borden, W. T. *J. Am. Chem. Soc.* **1998**, *120*, 3499.
(14) Galbraith, J. M.; Gaspar, P. P.; Borden, W. T. *J. Am. Chem. Soc.* **2002**, *124*, 11669.
(15) Kim, S.-J.; Hamilton, T. P.; Schaefer, H. F. *J. Am. Chem. Soc.* **1992**, *114*, 5349.
(16) Nakano, H. *J. Chem. Phys.* **1993**, *99*, 7983.
(17) Nakano, H. *Chem. Phys. Lett.* **1993**, *207*, 372.
(18) Nakano, H.; Hirao, K.; Gordon, M. S. *J. Chem. Phys.* **1998**, *108*, 5660.
(19) Hirao, K. *Chem. Phys. Lett.* **1992**, *190*, 374.
(20) Hirao, K. *Chem. Phys. Lett.* **1992**, *196*, 397.
(21) Hirao, K. *Int. J. Quantum Chem.* **1992**, *S26*, 517.
(22) Hirao, K. *Chem. Phys. Lett.* **1993**, *201*, 59.
(23) Andersson, K. *Theor. Chim. Acta* **1995**, *91*, 31.
(24) Andersson, K.; Roos, B. O. *Int. J. Quantum Chem.* **1993**, *45*, 591.
(25) Smith, B. A.; Cramer, C. J. *J. Am. Chem. Soc.* **1996**, *118*, 5490.
(26) Werner, H.-J.; Knowles, P. J. *J. Chem. Phys.* **1988**, *89*, 5803.
(27) Knowles, P. J.; Werner, H.-J. *Chem. Phys. Lett.* **1988**, *145*, 514.
(28) Langhoff, S. R.; Davidson, E. R. *Int. J. Quantum Chem.* **1974**, *8*, 61.
(29) Duch, W.; Diercksen, G. H. F. *J. Chem. Phys.* **1994**, *101*, 3018.
(30) MOLPRO is a package of ab initio programs written by Werner, H.-J. and Knowles, P. J. with contributions from the following: Amos, R. D.; Bernhardsson, A.; Berning, A.; Celani, P.; Cooper, D. L.; Deegan, M. J. O.; Dobbyn, A. J.; Eckert, F.; Hampel, C.; Hetzer, G.; Korona, T.; Lindh, R.; Lloyd, A. W.; McNicholas, S. J.; Manby, F. R.; Meyer, W.; Mura, M. E.; Nicklass, A.; Palmieri, P.; Pitzer, R.; Rauhut, G.; Schütz, M.; Stoll, H.; Stone, A. J.; Tarroni, R.; Thorsteinsson, T. Version 2000.1.
(31) Schmidt, M. W.; Baldridge, K. K.; Boatz, J. A.; Elbert, S. T.; Gordon, M. S.; Jensen, J. H.; Koseki, S.; Matsunaga, N.; Nguyen, K. A.; Su, S. J.; Windus, T. L.; Dupuis, M.; Montgomery, J. A. *J. Comput. Chem.* **1993**, *14*, 1347.
(32) Cabana, A.; Bachand, J.; Giguere, J. *Can. J. Phys.* **1974**, *52*, 1949.

Table 1. Relative Energies (in kcal mol^{-1}), Zero-Point Vibrational Energies (ZPVE, in kcal mol^{-1}), and Number of Imaginary Vibrational Frequencies (Nimag) of the Lowest-Energy States of Dehydrophenylnitrenes **3**−**5**, and Phenylnitrene (**8**) As Computed at the (*n*,*n*)-CASSCF/cc-pVTZ, MRMP2/cc-pVTZ, MRCI, and MRCI+Q Levels of Theory

species	*n*	state	CASSCF	ZPVE[a] (Nimag)	MRMP2[b]	MRCI[b,c]	MRCI+Q[b−d]	exp.
3	9	$^4A_2$	−284.03585	51.3 (0)	−285.03432	−284.80226	−284.99198	
	9	$^2A_2$	6.3	−0.3 (0)	5.3	0.7	1.9	
	9	$^2A_1$	42.9		34.1	28.9	28.7	
	9	$^2B_2$	22.7		34.4	21.9	21.3	
	9	$^2B_1$	66.9		62.1	*e*	*e*	
4	9	$^4A''$	3.7	−0.2 (0)	2.8	0.2	0.9	
	9	$^2A''$	−0.9	−0.5 (0)	−3.5	−0.7	−1.1	
	9	$^2A'$	42.8		32.3	29.9	29.5	
5	9	$^4A''$	0.6	0.0 (0)	0.6	0.2	0.3	
	9	$^2A''$	8.1	−0.3 (0)	7.9	3.3	4.4	
	9	$^2A'$	24.7		34.9	22.7	21.7	
8	8	$^3A_2$	−284.68416	59.6 (0)	−285.71404	−285.48170	−285.67792	
	8	$^1A_2$	17.1	−0.5 (0)	18.0	17.6	15.6	18.33 ± 0.69[f]
	8	$^1A_1$	40.8		33.2	29.9	29.2	30 ± 5[g]

[a] ZPVEs are given relative to the most stable state and were obtained at the (*n*,*n*)-CASSCF/cc-pVTZ level of theory. [b] Energies were computed at the (*n*,*n*)-CASSCF/cc-pVTZ optimized geometries. [c] Using a (3,3)- or (2,2)-CASSCF wave function as the multiconfiguration reference for **3**-**5** and **8**, respectively. This reduces to a single reference CISD for all quartet states and the $^{1,3}A_2$ states of phenylnitrene **8**. [d] Including Davidson correction. [e] The $^2B_1$ state cannot be described by this (3,3) active space. [f] Reference 35. [g] Reference 34.

Table 2. Bond Lengths (in Å) for the Species Considered in This Work As Computed at the (*n*,*n*)-CASSCF/cc-pVTZ Level of Theory

species	*n*	state	C–N	C1–C2	C2–C3	C3–C4	C4–C5	C5–C6	C6–C1
3	9	$^4A_2$	1.320	1.431	1.380	1.393			
	9	$^2A_2$	1.348	1.417	1.390	1.383			
	9	$^2A_1$	1.353	1.413	1.389	1.382			
	9	$^2B_2$	1.273	1.464	1.349	1.472			
	9	$^2B_1$	1.271	1.471	1.440	1.389			
4	9	$^4A''$	1.337	1.423	1.369	1.387	1.403	1.384	1.422
	9	$^2A''$	1.314	1.440	1.365	1.390	1.405	1.381	1.430
	9	$^2A'$	1.349	1.419	1.373	1.383	1.398	1.388	1.412
5	9	$^4A''$	1.321	1.412	1.377	1.396	1.411	1.376	1.434
	9	$^2A''$	1.348	1.412	1.361	1.414	1.390	1.394	1.412
	9	$^2A'$	1.279	1.487	1.452	1.358	1.458	1.343	1.467
6	6	$^1A_{1g}$		1.392					
7	7	$^2A_1$		1.380	1.396	1.394			
8	8	$^3A_2$	1.333	1.421	1.381	1.400			
	8	$^1A_2$	1.271	1.470	1.362	1.422			
	8	$^1A_1$	1.356	1.409	1.386	1.395			
9	5	$^2B_2$	1.267	1.471					

(1.380 Å) due to the higher s character of the bonds, while the other C−C bonds are slightly elongated (Table 2).

Phenylnitrene (**8**) is known from a number of experimental[33−35] and computational[11,12,15,36] investigations to have a triplet ground-state T_0 of A_2 symmetry. As the dehydrophenylnitrenes can be regarded as phenylnitrene derivatives, a closer look at some low-lying electronic states of **8** is warranted. A comparison of previous computational results for the different spin states of **8** can be found in a recent review by Karney and Borden.[37] In the T_0 state of **8**, the nonbonding n_y ($8b_2$) and n_x ($3b_1$) MOs are singly occupied, resulting in the $(8b_2)^1(3b_1)^1$ configuration (Figure 1).

The larger basis set used in our geometry optimization of **8** results in shortening of bonds between heavy atoms (Table 2 and Figure 2) by 0.004−0.005 Å as compared to the (8,8)-CASSCF/6-31G* data.[12,38] The next higher state of **8** is the lowest energy state on the singlet surface, S_0. This is an open-shell singlet with the same electron configuration as T_0, that is, $^1A_2$. The ΔE_{ST} between T_0 and S_0 is 18.33 ± 0.69 kcal mol^{-1} from negative ion photoelectron spectroscopy.[34,35] We obtain a classical energy difference of 18.0 kcal mol^{-1} at the MRMP2/

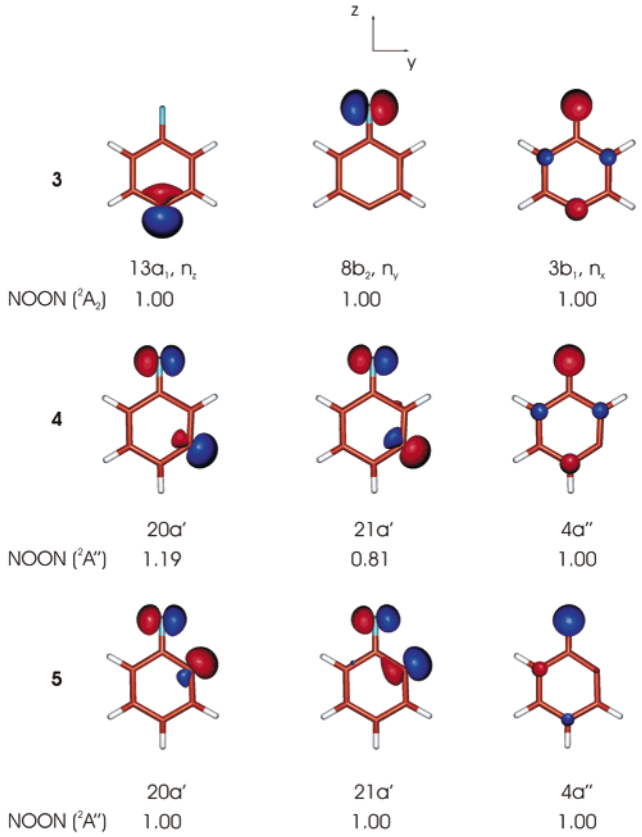

Figure 1. The nonbonding natural orbitals of the 4-, 3-, and 2-dehydrophenylnitrenes (**3**−**5**) as computed at the (9,9)-CASSCF/cc-pVTZ level of theory. The natural orbital occupation numbers of the lowest-energy doublet states are also given. Note that the $8b_2$ and $3b_1$ nonbonding natural orbitals of phenylnitrene (**8**) are qualitatively very similar.

(33) Smolinsky, G.; Wasserman, E.; Yager, W. A. *J. Am. Chem. Soc.* **1962**, *84*, 3220.
(34) Travers, M. J.; Cowles, D. C.; Clifford, E. P.; Ellison, G. B. *J. Am. Chem. Soc.* **1992**, *114*, 8699.
(35) McDonald, R. N.; Davidson, S. J. *J. Am. Chem. Soc.* **1993**, *115*, 10857.
(36) Castell, O.; García, V. M.; Bo, C.; Caballol, R. *J. Comput. Chem.* **1996**, *17*, 42.
(37) Karney, W. L.; Borden, W. T. In *Advances in Carbene Chemistry*; Brinker, U. H., Ed.; Elsevier: Amsterdam, 2001; Vol. 3, p 205.
(38) Liu, R.; Zhou, X. *Chem. Phys. Lett.* **1993**, *207*, 185.

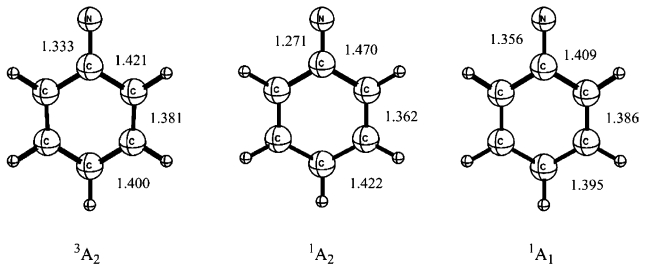

Figure 2. Structures of T_0, S_0, and S_1 states of phenylnitrene as computed at the CASSCF/cc-pVTZ level of theory. Important bond lengths are given in Å.

Table 3. Summary of the States Possible by Distributing Three Electrons among Three Nonbonding Orbitals

	occupation			**3**	**4**, **5**	
character	σ(C)	σ(N)	π(N)	C_{2v}	C_s, planar	C_s, nonplanar
triradical	1	1	1	A_2	A″	A″
carbene/iminyl	2	1	0	B_2	A′	A″
nitrene/phenyl radical	1	2	0	A_1	A′	A′
	1	0	2	A_1	A′	A′
zwitterions/π (N)	2	0	1	B_1	A″	A′
radical[a]	0	2	1	B_1	A″	A′

[a] The lowest energy $^2B_1$ state is a triradical involving a singly occupied benzene π MO.

cc-pVTZ//(8,8)-CASSCF/cc-pVTZ level, while a value of 17.5 kcal mol^{-1} is obtained after inclusion of ZPVE. A slightly lower classical energy difference of 15.6 kcal mol^{-1} is obtained at the CISD+Q/cc-pVTZ level of theory. Previous CISD+Q/DZ+d//CISD/DZ+d computations by Kim et al.[15] arrive at a classical singlet−triplet energy gap (18.3 kcal mol^{-1}) closer to experiment despite using a smaller basis set.

Two even higher-lying singlet states of **8**, S_1 and S_2, are reached by $n_x(3b_1) \rightarrow n_y(8b_2)$ or $n_y(8b_2) \rightarrow n_x(3b_1)$ transitions, respectively. Both states have closed shells, but two configurations contribute strongly to these $^1A_1$ states.[12,15] The S_1 electronic state of **8** is found to be higher in energy by 33.2 kcal mol^{-1} (MRMP2) or 29.2 kcal mol^{-1} (MRCI+Q) in the present work. This is in good agreement with the 30 ± 5 kcal mol^{-1} experimental estimate by Travers et al.[34] and with previous computational data.[11,12,15,25,36] The S_2 state is not considered further in this work. In the following paragraphs, we will discuss the electronic states of dehydrophenylnitrenes as variations on the phenylnitrene theme.

B. General Considerations for Dehydrophenylnitrenes. In addition to the nitrogen-centered nonbonding orbitals of phenylnitrene, dehydrophenylnitrenes possess σ nonbonding orbitals located at the dehydro carbon atoms (Figure 1). There are seven ways to occupy these MOs with three electrons (Table 3).

One of the resulting states is a triradical quartet, but a triradical doublet is also possible. These states have A_2 symmetry. The remaining states are doublets, and, depending on the occupation of the nonbonding MOs, these can be classified as having closed-shell carbene and iminyl radical, closed-shell nitrene and phenyl radical, or zwitterion and π(N) radical characters (Chart 2). These latter states transform according to the B_2, A_1, and B_1 irreducible representations in the C_{2v} molecular framework of **3**. As is discussed below, the zwitterions/π(N) radical state is, however, not the lowest-energy

Chart 2. Lewis Structures of the Triradical, Carbene/Iminyl Radical, Nitrene/Phenyl Radical, and Planar Allene/2-Iminylpropane-1,3-diyl States of 4-Dehydrophenylnitrene **3**[a]

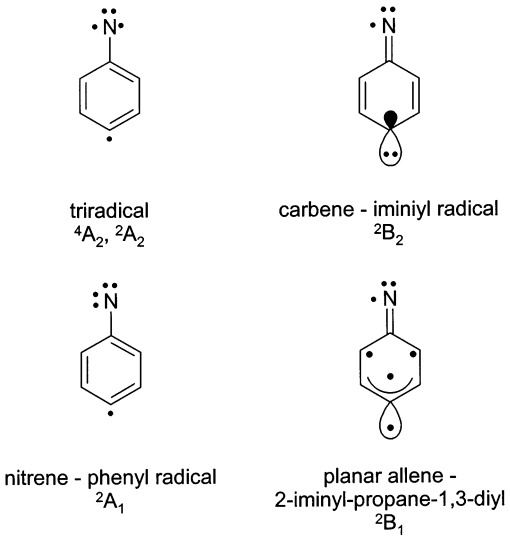

[a] Two dots next to each other represent an electron pair.

$^2B_1$ state of **3**: a planar allene/2-iminyl propa-1,3-diyl species is found to be lower in energy.

Reduction of the symmetry to planar C_s as in **4** and **5** allows for mixing of states, and we have limited ourselves here to the lowest-energy A′ and A″ states of **4** and **5**.

C. 4-Dehydrophenylnitrene. The configurations of the electronic states of 4-dehydrophenylnitrene considered in this work are as follows:

$...(1b_1)^2(12a_1)^2(7b_2)^2(2b_1)^2(1a_2)^2(8b_2)^1(13a_1)^1(3b_1)^1$	$^4A_2$, $^2A_2$	
$...(1b_1)^2(12a_1)^2(7b_2)^2(2b_1)^2(1a_2)^2\,(8b_2)^1(13a_1)^2$	$^2B_2$	$n_x(3b_1) \rightarrow n_z(13a_1)$
$...(1b_1)^2(12a_1)^2(7b_2)^2(2b_1)^2(1a_2)^2(8b_2)^2(13a_1)^1$	$^2A_1$	$n_x(3b_1) \rightarrow n_y(8b_2)$

The $8b_2$ and $3b_1$ MOs are largely p AO-type and centered at the nitrogen atom as already discussed for phenylnitrene (Figure 1). The $13a_1$ MO is of sp^2-type and located at C4 (Figure 1). The doubly occupied $1b_1$, $2b_1$, and $1a_2$ are the π orbitals of the phenyl system. These six MOs, together with the three antibonding phenyl π orbitals − $2a_2$, $4b_1$, and $5b_1$ − comprise the active space in the CASSCF computations.

In the electronic ground state of the molecule, the three unpaired electrons are high-spin coupled, resulting in a quartet state of A_2 symmetry ($\tilde{X}$ $^4A_2$). The lowest-energy state in the doublet manifold (ã $^2A_2$) has the same electron configuration as the quartet ground state; just the coupling of electron spins is different. The excitation energy from the quartet ground state to the ã $^2A_2$ state is 5.3 kcal mol^{-1} (see Table 1, Figure 3).

This excitation energy is much smaller than that in **8** (18 kcal mol^{-1}), although the states involved are analogous ($^3A_2 \rightarrow {}^1A_2$). The reason for the smaller excitation energy in **3** can be found upon considering how the spins of its three electrons are coupled. In $^1A_2$-**8**, the two electrons confined to the $3b_1$ and $8b_2$ MOs have antiparallel spins. These electrons have, therefore, a larger Coulomb repulsion than they have in the triplet state; a sizable excitation energy of 18 kcal mol^{-1} is the consequence.[39,40] On the other hand, these electrons can remain high-spin coupled in $^2A_2$-**3** if the electron described by $13a_1$ has its spin aligned in the opposite direction, as then the overall

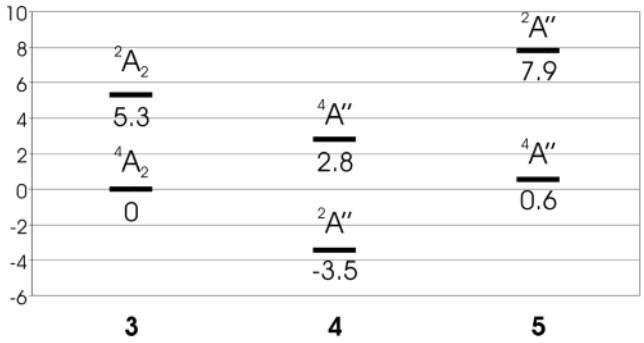

Figure 3. Graphical representation of the energies (in kcal mol^{-1}) of the lowest-lying spin states of 4-, 3-, and 2-dehydrophenylnitrene (**3**−**5**) as computed at the MRMP2/cc-pVTZ//(9,9)-CASSCF/cc-pVTZ level of theory.

spin multiplicity is two. This arrangement avoids the larger Coulomb repulsion between the $3b_1$ and $8b_2$ electrons located at the nitrogen center with antiparallel spins as found in $^1A_2$-**8**. As the $3b_1$ orbital only has a small coefficient at C4 while the $8b_2$ and the $13a_1$ MOs are disjoint, that is, have no atoms in common, the Coulomb repulsion resulting from electrons with antiparallel spins is much smaller in $^2A_2$-**3**. Hence, the excitation energy to $^2A_2$-**3** is lower than that to $^1A_2$-**8** from the respective ground state. Indeed, the $^4A_2 \rightarrow {}^2A_2$ excitation energy of 5 kcal mol^{-1} is remarkably close to the singlet−triplet energy splitting in α,4-dehydrotoluene (5−7 kcal mol^{-1}, correlation consistent CI and difference-dedicated CI2).[41,42] The triplet ground state of the latter has an electronic configuration, $(b_1)^1(a_1)^1$, involving MOs similar to those of $^2A_2$-**3**.

Both A_2 states are minima on the C_6H_4N potential energy surfaces at the (9,9)-CASSCF/cc-pVTZ level of theory. The geometries of these two states are similar to that of $^3A_2$ phenylnitrene ($^3A_2$-**8**) (Figures 2 and 4) and show only minor bond length alternation ($\Delta r = 0.051$ Å).

The geometry of the $^2A_2$ state, however, differs significantly from that of $^1A_2$-**8**. For example, the C−N distance in $^2A_2$ is longer than that in $^4A_2$ by 0.028 Å, while it is shorter by 0.062 Å in $^1A_2$-**8** as compared to $^3A_2$-**8**. This further corroborates the analysis of the electronic structure that the lowest-energy low-spin A_2 states of **3** and **8** are of different character. Comparing the structures of $^4A_2$-**3** and $^2A_2$-**3** with $^3A_2$-**8**, the largest difference in bond lengths is found for the C−N bond, which is 0.013 Å shorter in $^4A_2$-**3** and 0.015 Å longer in $^2A_2$-**3** than in $^3A_2$-**8**. The same trend, shortening of the exocyclic bond in the high-spin and lengthening of it in the low-spin state, is also found in the benzyl radical−α,4-dehydrotoluene pair.[41] It has been explained by Wenthold et al. by $\sigma-\pi$ exchange interactions, which are favorable in the high-spin state and maximized by shortening of the exocyclic bond through enhanced π conjugation. The enhanced Coulomb repulsion in the low-spin state is minimzed by reducing π conjugation, which is achieved by bond elongation.[41] The same arguments can be used to explain the bond length pattern in the **3**−**8** system.

The $^2A_1$ and $^2B_2$ excited states (not depicted in Figure 3) of **3** are obtained from the doublet ground state of A_2 symmetry

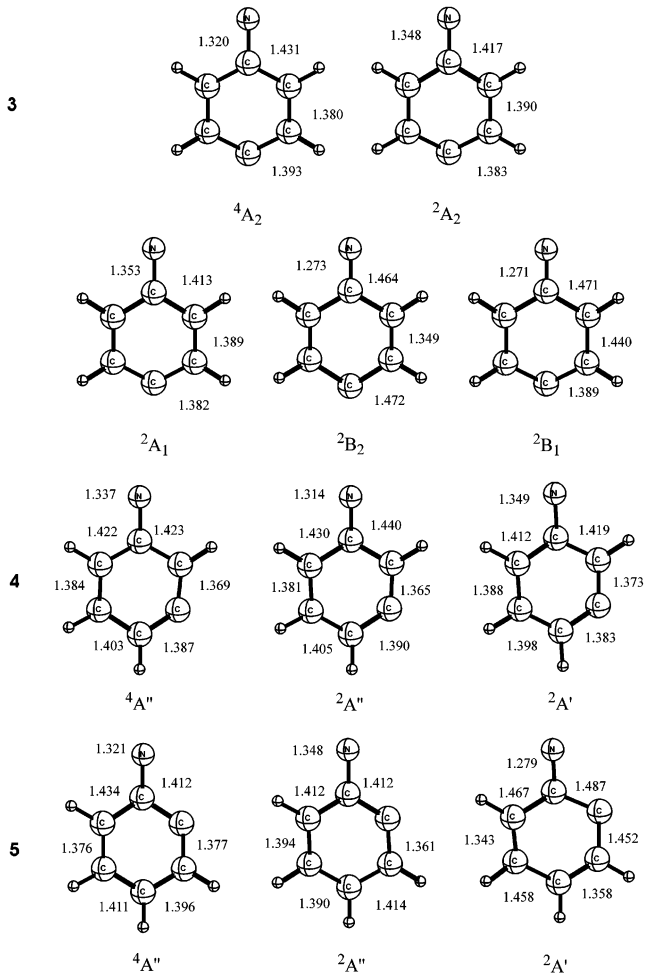

Figure 4. Structures of the electronic states of dehydrophenylnitrenes (**3**−**5**) considered in this work as computed at the (9,9)-CASSCF/cc-pVTZ level of theory. Important bond lengths are given in Å.

by exciting one electron from the $3b_1$ π MO, largely located at the nitrogen atom, into the σ symmetric (with respect to the ring plane) $8b_2$ or $13a_1$ MOs, respectively. The $^2B_2$ state resulting from a $n_x(3b_1) \rightarrow n_z(13a_1)$ transition has no equivalent in phenylnitrene. It can be considered as having a closed-shell carbene moiety at C4 (doubly occupied $13a_1$ MO) combined with an iminyl radical and thus resembles a singlet cyclohexadienylidene (Chart 2). Its computed geometry is in agreement with this descriptive Lewis structure. There is pronounced bond length alternation in the six-membered ring, 1.349−1.471 Å, while the C−N distance (1.273 Å) is significantly shorter than that in $^4A_2$ (1.320 Å).

The CASSCF natural orbitals and their occupation numbers also reflect the carbene character of $^2B_2$-**3**. The $3b_1$ MO has its largest coefficient on C4 rather than on nitrogen (Figures 1 and 5). The natural orbital occupation numbers (NOON) of the $13a_1$ and $3b_1$ MOs are 1.92 and 0.07, indicative of a typical closed-shell carbene. While the MRCI+Q energies relative to $^4A_2$-**3** are, in general, in agreement with the MRMP2 data for all states of **3**−**5** considered (Table 1), this is not the case for the $^2B_2$ state of **3**. Rather, the excitation energy to the $^2B_2$ state depends strongly on the level of theory employed. While it is computed to lie 22.7 kcal mol^{-1} higher than $^4A_2$ at (9,9)-CASSCF/cc-pVTZ, this energy difference increases to 34.4 kcal mol^{-1} at the MRMP2 level. On the other hand, the MRCI+Q excitation

(39) Hrovat, D. A.; Borden, W. T. In *Modern Electronic Structure Theory and Applications in Organic Chemistry*; Davidson, E. R., Ed.; World Scientific: Singapore, 1997; p 171.
(40) Borden, W. T.; Iwamura, H.; Berson, J. A. *Acc. Chem. Res.* **1994**, *27*, 109.
(41) Wenthold, P. G.; Wierschke, S. G.; Nash, J. J.; Squires, R. R. *J. Am. Chem. Soc.* **1994**, *116*, 7378.
(42) Cabrero, J.; Ben-Amor, N.; Caballol, R. *J. Phys. Chem. A* **1999**, *103*, 6220.

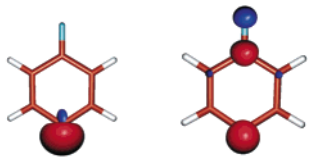

Figure 5. The $13a_1$ and $3b_1$ nonbonding natural orbitals of the $^2B_2$ state of 4-dehydrophenylnitrene (**3**) as computed at the (9,9)-CASSCF/cc-pVTZ level of theory. Note the large coefficient on C4 in $3b_1$ and the antibonding character between C1 and N. The natural orbital occupation numbers are also given.

energy is 21.3 kcal mol^{-1}, in good agreement with both (9,9)-CASSCF and (3,3)-CASSCF (21.5 kcal mol^{-1}) data. Hence, it appears that the MRMP2 method overestimates the stability of the $^4A_2$ state relative to the $^2B_2$ state, which has marked closed-shell singlet carbene character. The behavior of the MRMP2 method observed here parallels the well-known tendency of CASPT2 to overestimate the stability of some open-shell states.[12,23−25]

In C_s symmetry (mirror plane perpendicular to the ring plane), the $^2B_2$ and $^2A_2$ states both are A″ (see Table 3). A state-averaged (9,9)-CASSCF/cc-pVTZ calculation at the $^2B_2$-**3** geometry places the $^2A_2$ state 13 kcal mol^{-1} lower in energy. As detailed above (Theoretical Methods), we have not computed second derivatives for higher-lying electronic states. Note, however, that it is well known that the closed-shell singlet states ($^1A_1$) of both 4-oxo-2,5-cyclohexadienylidene[2,43] and cyclopentadienylidene[44,45] correspond to saddle points in C_{2v} molecular point group symmetry, with puckered rings being more stable.

The $^2A_1$-**3** state results from the same $n_x(3b_1) \rightarrow n_y(8b_2)$ transition as the $^1A_1$ state (S_1) of **8**. It thus resembles a combination of the $^2A_1$ ground state of the phenyl radical (**7**) and $^1A_1$-**8**. The NOON values of the $8b_2$ and $3b_1$ MOs are 1.61 and 0.42, respectively. The adiabatic excitation energy from $^4A_2$-**3** to $^2A_1$-**3** is 34.1 kcal mol^{-1} at MRMP2 and 28.7 kcal mol^{-1} at MRCI+Q. The discrepancy between MRCI+Q and MRMP2 is not as dramatic as that for the $^2B_2$ state; however, an overestimation of the excitation energy at MRMP2 is possible. Nonetheless, an excitation energy of around 30 kcal mol^{-1} is similar to the T_0-S_1 energy difference in **8** (33.2 kcal mol^{-1} at MRMP2 and 29.2 kcal mol^{-1} at MRCI+Q). The geometry of $^2A_1$-**3** is very similar to that of $^1A_1$-**8**. For example, the C−N distance is only 0.003 Å shorter in the dehydro species. The analogy to **8** suggests that another excited $^2A_1$ state should be accessible by a $n_x(8b_2) \rightarrow n_y(3b_1)$ excitation (resembling S_2 of **8**), which is expected to be higher in energy and which is not considered in this work.[15]

We finally consider $^2B_1$ states of **3**. The adiabatic excitation energy from the $^4A_2$-**3** to the lowest-energy $^2B_1$ state of **3** is a sizable 62.1 kcal mol^{-1} (Table 1). The NOON values of $^2B_1$-**3** (Figure 6) deviate strongly from the expectations for a zwitterion−π(N) radical anticipated above (Table 3).

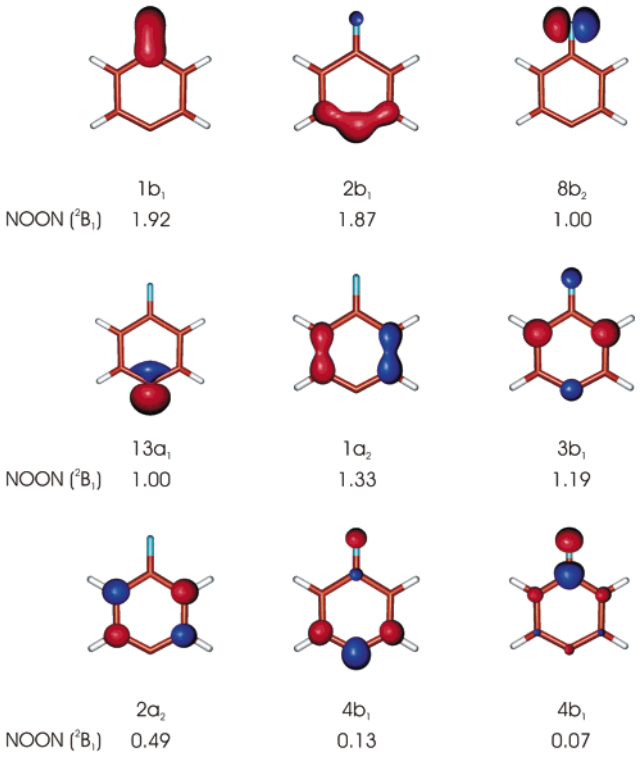

Figure 6. Natural orbitals and their occupation numbers of the lowest-energy $^2B_1$ state of 4-dehydrophenylnitrene (**3**) as computed at the (9,9)-CASSCF/cc-pVTZ level of theory.

Inspection of the CASSCF wave function shows a $(8b_2)^1(13a_1)^1(1a_2)^1$ leading configuration indicative of a triradical species. It may be viewed (see Figure 3 for structural data) as a combination of a planar allene ($^1A_2$)[46,47] and a azatrimethylenemethane-like unit ($^1A_1$)[48] combined with a σ(N) radical ($^1B_2$), that is, a 2-iminylpropane-1,3-diyl unit (see Chart 2). The $^2B_2$ state of free 2-iminylpropane-1,3-diyl (C_3H_4N, **9**) indeed has a very similar geometry: r(CN) = 1.267 Å and r(CC) = 1.471 Å at the analogous level of theory [(5,5)-CASSCF/cc-pVTZ]. A second doublet state arising from the $(8b_2)^1(13a_1)^1(1a_2)^1$ configuration is found from a SA-CASSCF/cc-pVTZ computation to be 5 kcal mol^{-1} higher in energy, while the second excited state is 60 kcal mol^{-1} above $^2B_1$-**3**. Note that the diradical states in planar allene[46,47] and in 2-cyclohexadiene[49,50] also are more favorable than closed-shell zwitterions.

D. 3- and 2-Dehydrophenylnitrene. The molecular point group symmetry of these molecules is reduced to C_s. As the in-plane nonbonding MOs at nitrogen and at the carbon radical site transform both according to the same irreducible representation (a′), they can interact, giving rise to two new orbitals depicted in Figure 1. The electronic configurations of the lowest-energy quartet (^{4}A″) states of **4** and **5** are thus as follows: $...(1a'')^2(2a'')^2(3a'')^2(20a')^1(21a')^1(4a'')^1$.

(43) Solé, A.; Olivella, S.; Bofill, J. M.; Anglada, J. M. *J. Phys. Chem.* **1995**, *99*, 5934.
(44) Bofill, J. M.; Bru, N.; Farràs, J.; Olivella, S.; Solé, A.; Vilarrasa, J. *J. Am. Chem. Soc.* **1988**, *110*, 3740.
(45) Collins, C. L.; Davy, R. D.; Schaefer, H. F. *Chem. Phys. Lett.* **1990**, *171*, 259.
(46) Bettinger, H. F.; Schreiner, P. R.; Schleyer, P. v. R.; Schaefer, H. F. *J. Phys. Chem.* **1996**, *100*, 16147.
(47) Jackson, W. M.; Mebel, A. M.; Lin, S. H.; Lee, Y. T. *J. Phys. Chem. A* **1997**, *101*, 6638.
(48) Li, J.; Worthington, S. E.; Cramer, C. J. *J. Chem. Soc., Perkin Trans. 2* **1998**, 1045.
(49) Angus, R. O., Jr.; Schmidt, M. W.; Johnson, R. P. *J. Am. Chem. Soc.* **1985**, *107*, 532.
(50) Engels, B.; Schöneboom, J. C.; Münster, A. F.; Groetsch, S.; Christl, M. *J. Am. Chem. Soc.* **2002**, *124*, 287.

Scheme 3. Isodesmic Equations for the Evaluation of the Interaction of Phenylnitrene and Phenyl Radical Moieties in the Quartet States of Dehydrophenylnitrenes As Computed at the MRMP2/cc-pVTZ//CASSCF/cc-pVTZ + ZPVE Level of Theory

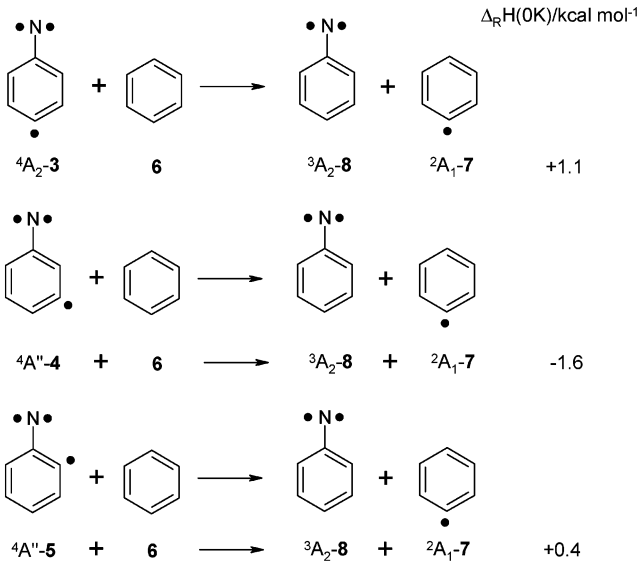

The quartet states of **4** and **5** considered here correspond to minima on the C_6H_4N PES. They have bond lengths similar to those of $^3A_2$-**8**, only the C−C bonds about the dehydrocarbon atoms are shorter due to their increased s character. The geometries (Figure 4) also show modest bond length alternation ($\Delta r \leq 0.058$ Å) and C−N distances similar to those in $^4A_2$-**3**.

Among the three quartet dehydrophenylnitrenes, $^4A_2$-**3** is found to be the most stable, while $^4A''$-**4**, 2.8 kcal mol^{-1} above $^4A_2$-**3** in energy, is the least stable (Figure 3). The 0.6 kcal mol^{-1} energy difference between $^4A_2$-**3** and $^4A''$-**5** is very small, making these two dehydrophenylnitrenes almost isoenergetic. The same energetic ordering of quartet dehydrophenylnitrenes is obtained at CISD+Q/cc-pVTZ, but the energy differences are found to be smaller: 0.9 kcal mol^{-1} (**4**) and 0.3 kcal mol^{-1} (**5**) with respect to $^4A_2$-**3**.

The isodesmic equations depicted in Scheme 3 probe the stabilities of the triradicals with respect to separation into triplet phenylnitrene ($^3A_2$-**8**) and phenyl radical ($^2A_1$-**7**); a positive heat of reaction indicates a stabilization of the triradical. A destabilization of the triradical is only observed for the least stable $^4A''$-**4**.

We now turn our attention to the doublet states of **4** and **5**. The electronic structure of $^2A''$-**5** is characterized by occupation numbers of 1.00 and 1.00 for the two natural orbitals of a′ symmetry (Figure 1). On the other hand, the NOON values of these 20a′ and 21a′ orbitals are 1.19 and 0.81 for $^2A''$-**4**, respectively. This indicates that one of the $\sigma^2\pi^1$ configurations dominates the wave function in $^2A''$-**4**. Indeed, the weights of reference configurations in the MRCI wave functions are 40% $[(20a')^2(21a')^0(4a'')^1]$, 26% $[(20a')^0(21a')^2(4a'')^1]$, and 18% $[(20a')^1(21a')^1(4a'')^1]$ for $^2A''$-**4**, but 31% $[(20a')^2(21a')^0(4a'')^1]$, 31% $[(20a')^0(21a')^2(4a'')^1]$, and 20% $[(20a')^1(21a')^1(4a'')^1]$ in the case of $^2A''$-**5**. The energy gap between $^2A''$ and $^4A''$ of **4** is −6.3 kcal mol^{-1} in favor of the doublet state, while an energy splitting of 7.3 kcal mol^{-1} is obtained between the $^2A''$ and $^4A''$ states of **5** in favor of the quartet state. This trend is confirmed by the MRCI+Q data, which are −2.0 and +4.1 kcal mol^{-1} for the energy gaps in **4** and **5**, respectively. A difference in the 3−4 kcal mol^{-1} range between MRMP2 and MRCI+Q is also obtained for the energy splitting of the lowest-energy quartet and doublet state of **3** (Table 4). This difference is not solely due to the smaller active spaces used in the MRCI+Q computations, as gaps of 4.2 (**3**), −4.8 (**4**), and 6.3 kcal mol^{-1} (**5**) result if the MRMP2 evaluation is based on (3,3) active spaces (Table 4).

Table 4. The Classical Energy Difference between Doublet and Quartet States (in kcal mol^{-1}) in Dehydrophenylnitrenes **3**−**5** As Computed at Various Levels of Theory[a]

methods	3	4	5
(9,9)-CASSCF/cc-pVTZ	6.3	−4.6	7.5
(9,9)-MRMP2/cc-pVTZ[b,c]	5.3	−6.3	7.3
(3,3)-MRMP2/cc-pVTZ[b,d]	4.2	−4.8	6.3
MRCI/cc-pVTZ[b,d]	0.7	−0.9	3.1
MRCI+Q/cc-pVTZ[b,d]	1.9	−2.0	4.1

[a] A negative value indicates that the doublet is more stable than the quartet state. [b] Using the (9,9)-CASSCF/cc-pVTZ geometries. [c] Based on the (9,9)-CASSCF wave function. [d] Based on the (3,3)-CASSCF wave function.

The $^2A''$-**4** state behaves differently not only in energetic and electronic but also in geometric structural aspects. It has a significantly larger bond length alternation of 0.075 Å, a rather short C−N, and a rather long C−C bond as compared to those of $^2A''$-**5** and $^2A_2$-**3** (Figure 4). The pattern of bond shortening and elongation is typical of systems which profit from through-bond interaction (TBI) between lobes of nonbonding orbitals and an intervening σ^* orbital.[51−53] The participation of the C1−C2 bond in TBI results in its elongation to 1.440 Å, which is significantly longer than that in the corresponding quartet state (1.420 Å) and in the phenyl radical (1.396 Å). On the other hand, the flanking bonds are shortened (C−N, 1.314 Å; C2−C3, 1.365 Å) due to the bonding interaction of the lobes at N and C3 with σ^*(C1−C2). The 20a′ MO profits from the bonding interaction with σ^* and is thus lowered in energy. As a consequence thereof, the 20a′ occupation number is increased, and a $(20a')^2(4a'')^1$ configuration dominates the wave function. In the high-spin state, $(20a')^1(21a'')^1(4a')^1$, there is no net stabilization by through-bond interaction. The leading configuration of the $^2A''$-**4** state is $(20a')^2(4a'')^1$, and that of the quartet state is $(20a')^1(21a'')^1(4a')^1$. As two different configurations are involved, the lower energy of $^2A''$-**4** should not be considered a violation of Hund's rule. However, the $^2A''$ state ground state also has a significant contribution from the $(20a')^1(21a')^1(4a'')^1$ configuration (18%). In analogy to α,3-dehydrotoluene,[39,41] spin-polarization[54] of the $(20a')^1(21a')^1(4a'')^1$ configuration will also tend to favor the low-spin over the high-spin state.

The lowest-energy $^2A'$ state of **4** has closed-shell nitrene/phenyl radical character (Table 3, Charts 2 and 3), as indicated by the NOON values of 1.0 for σ(C), 1.6 for σ(N), and 0.4 for π(N), which are very similar to those of $^2A_1$-**3**. Also, the geometry obtained for $^2A'$-**4** is very similar to that of $^2A_1$-**3** (Figure 4). The $^2A'$-**4** state lies higher in energy than the quartet state by 29.5 kcal mol^{-1}. As was already discussed for $^2A_1$-**3**, the CASSCF energies are somewhat higher than the MRMP2 data (Table 1). While the closed-shell carbene/iminyl radical

(51) Hoffmann, R.; Imamura, A.; Hehre, W. J. *J. Am. Chem. Soc.* **1968**, *90*, 1499.
(52) Jordan, K. D. *Theor. Chem. Acc.* **2000**, *103*, 286.
(53) Gleiter, R. *Angew. Chem.* **1974**, *86*, 770; *Angew. Chem., Int. Ed. Engl.* **1974**, *13*, 696.
(54) Kollmar, H.; Staemmler, V. *Theor. Chim. Acta* **1978**, *48*, 223.

Chart 3. The Lowest-Energy $^2A'$ States of **4** and **5** Have Closed-Shell Nitrene/Phenyl Radical Character and Carbene/Iminyl Radical Character, Respectively

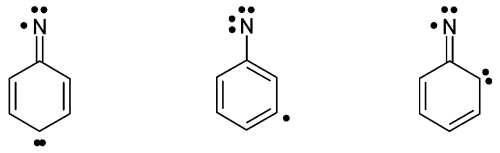

$^2B_2$-**3** $^2A'$-**4** $^2A'$-**5**

($^2B_2$) is more favorable than the closed-shell nitrene/phenyl radical ($^2A_1$) for **3**, this appears not to be the case for **4**. The meta orientation of the dehydro carbon atom and the exocyclic nitrogen in **4** prohibits formation of the three double bonds of a carbene/iminyl radical structure (Chart 3). This, however, is possible for **5**, and, consequently, the lowest-energy $^2A'$ state of **5** has carbene/iminyl character.

The $^2A'$-**5** carbene/iminyl radical is only 0.4 kcal mol^{-1} (MRCI+Q) less stable than $^2B_2$-**3**. As was already discussed for the latter, the MRMP2 energy of $^2A'$-**5** is considerably higher than the CASSCF and the MRCI(+Q) results.

Summary and Conclusions

The electronic and geometric structures of 4-, 3-, and 2-dehydrophenylnitrenes (**3**−**5**) have been studied using the (9,9)-MRMP2/cc-pVTZ and (3,3)-MRCI+Q/cc-pVTZ methods on geometries optimized at the (9,9)-CASSCF/cc-pVTZ level of theory. The quartet states of dehydrophenylnitrenes are found to lie energetically within 1 kcal mol^{-1} (MRCI+Q) or 3 kcal mol^{-1} (MRMP2). The lowest-energy doublet state of **3** has the same electronic configuration (A_2 symmetry) as the quartet ground state. The doublet-quartet energy splitting is only 2−5 kcal mol^{-1} for **3** but 4−7 kcal mol^{-1} for **5** ($^2A''$ and $^4A''$). Additional energetically higher-lying doublet states were investigated for **3**: $^2B_2$ is 21 kcal mol^{-1} (MRCI+Q), $^2A_1$ is 29−34 kcal mol^{-1}, and $^2B_1$ is 62 kcal mol^{-1} above the $^4A_2$ ground state. The $^2B_2$ state has strong closed-shell carbene character, resulting in an overestimated excitation energy from $^2A_2$ at the MRMP2 level.

The 3-dehydrophenylnitrene (**4**) system behaves exceptionally. It prefers a doublet over a quartet ground state by −2 (MRCI+Q) to −6 (MRMP2) kcal mol^{-1}. The structure of $^2A''$-**4** is more distorted than those of the other low-energy doublet states, in agreement with through-bond interaction involving the in-plane orbital lobes at N and C3 and the intervening elongated C−C bond.

We have shown that for the seemingly simple dehydrophenylnitrene system a delicate competition between ferromagnetic (quartet, $S = {}^3/_2$) and antiferromagnetic (doublet, $S = {}^1/_2$) coupling of electron spins is possible. With one spin-carrying orbital being orthogonal to two coplanar orbitals, the relative orientation of the latter orbitals at the phenyl coupling unit (ortho, meta, or para) determines which mode of electron coupling prevails. Through-bond interaction provides a mechanism for low-spin coupling if the coplanar orbitals are in the meta orientation.

Acknowledgment. This work was financially supported by the Fonds der Chemischen Industrie and the Deutsche Forschungsgemeinschaft. H.F.B greatly appreciates support from the Fonds der Chemischen Industrie through a Liebig Fellowship. We thank Dr. H.-H. Wenk and M. Winkler for helpful discussions.

Supporting Information Available: Cartesian coordinates, absolute energies, and harmonic vibrational frequencies for all stationary points computed in this paper (PDF). This material is available free of charge via the Internet at http://pubs.acs.org.

JA029296U